

Journal of Visualized Experiments

Functional interrogation of adult hypothalamic neurogenesis with focal radiological inhibition.

--Manuscript Draft--

Manuscript Number:	JoVE50716R2
Article Type:	Invited Methods Article - JoVE Produced Video
Corresponding Author:	Daniel Allen Lee, Ph.D. California Institute of Technology Pasadena, CA UNITED STATES
First Author:	Daniel Allen Lee, Ph.D.
Order of Authors:	Daniel Allen Lee, Ph.D. Juan Salvatierra Esteban Velarde John Wong Eric C Ford, Ph.D. Seth Blackshaw, Ph.D.
Abstract:	<p>The functional characterization of adult-born neurons remains a significant challenge. Approaches to inhibit adult neurogenesis via invasive viral delivery or transgenic animals have potential confounds that make interpretation of results from these studies difficult. New radiological tools are emerging, however, that allow one to non-invasively investigate the function of select groups of adult-born neurons through accurate and precise anatomical targeting in small animals. Focal ionizing radiation inhibits the birth and differentiation of new neurons, and allows targeting of specific neural progenitor regions. In order to illuminate the potential functional role that adult hypothalamic neurogenesis plays in the regulation of physiological processes, we developed a non-invasive focal irradiation technique to selectively inhibit the birth of adult-born neurons in the hypothalamic median eminence. We describe a small animal radiation research platform (SARRP) developed by our group, and a method for computer tomography imaging with arc beam radiation delivery to enable precise and accurate anatomical targeting in small animals. This SARRP protocol described herein uses three-dimensional volumetric image guidance for localization and targeting of the radiation dose, minimizes radiation exposure to non-targeted brain regions, and allows for conformal dose distribution with sharp beam boundaries. This protocol allows one to ask questions regarding the function of adult-born neurons, but also opens areas to questions in areas of radiobiology, tumor biology, and immunology. These new radiological tools will facilitate the translation of discoveries at the bench to the bedside.</p>

April 30, 2013

Dr. Michelle Kinahan, Ph.D.
Science Editor
Journal of Visualized Experiments

Dear Dr. Kinahan,

Thank you very much for your recent letter regarding our manuscript JoVE50716R1 'Functional interrogation of adult hypothalamic neurogenesis with focal radiological inhibition'. We are delighted that both you and the Reviewers consider our work of interest for the Journal of Visualized Experiments, and have rewritten the manuscript to address reviewer comments. We have re-arranged the figures as requested by the reviewers, and addressed all comments below, with our responses in bold font. The use of this approach for selective irradiation of neurogenic niches may have significant implications in revealing the functional role of new adult-born neurons on physiology and disease. Furthermore, the possibility for conceptual advance in multiple research disciplines is enhanced by the introduction and detailed description of this technique.

Sincerely,

Daniel Lee, Ph.D.
California Institute of Technology

Seth Blackshaw, Ph.D.
Johns Hopkins School of Medicine

Title: Functional interrogation of adult hypothalamic neurogenesis with focal radiological inhibition.

Authors:

Daniel A. Lee^{1,2*}, Juan Salvatierra², Esteban Velarde³, John Wong³, Eric Ford⁴, Seth Blackshaw^{2,5*}

¹Division of Biology, California Institute of Technology, Pasadena, California 91125, USA

²Solomon H. Snyder Department of Neuroscience, Neurology, and Ophthalmology, Johns Hopkins University School of Medicine, Baltimore, Maryland 21205, USA

³ Department of Radiation Oncology & Molecular Radiation Sciences, Johns Hopkins University School of Medicine, Baltimore, Maryland 21231, USA

⁴ Department of Radiation Oncology, University of Washington Medical Center, Seattle, Washington 98195, USA

⁵ Institute for Cell Engineering and High-Throughput Biology Center, Johns Hopkins University School of Medicine, Baltimore, Maryland 21205, USA.

* Address all correspondence to Daniel A. Lee (leed@caltech.edu; Tel: +443 955 8535) and Seth Blackshaw (sblack@jhmi.edu; Tel: 410 614 9568)

Key Words: Neurogenesis, Irradiation, Radiological treatment, Computer-tomography (CT) imaging, Hypothalamus, Hypothalamic Proliferative Zone (HPZ), Median Eminence (ME), Small Animal Radiation Research Platform (SARRP)

Short Abstract

The function of adult-born mammalian neurons remains an active area of investigation. Ionizing radiation inhibits the birth of new neurons. Using computer tomography-guided focal irradiation (CFIR), three-dimensional anatomical targeting of specific neural progenitor populations can now be used to assess the functional role of adult neurogenesis.

Long Abstract

The functional characterization of adult-born neurons remains a significant challenge. Approaches to inhibit adult neurogenesis via invasive viral delivery or transgenic animals have potential confounds that make interpretation of results from these studies difficult. New radiological tools are emerging, however, that allow one to non-invasively investigate the function of select groups of adult-born neurons through accurate and precise anatomical targeting in small animals. Focal ionizing radiation inhibits the birth and differentiation of new neurons, and allows targeting of specific neural progenitor regions. In order to illuminate the potential functional role that adult hypothalamic neurogenesis plays in the regulation of physiological processes, we developed a non-invasive focal irradiation technique to selectively inhibit the birth of adult-born neurons in the hypothalamic median eminence. We describe a method for Computer tomography-guided focal irradiation (CFIR) delivery to enable precise and accurate anatomical targeting in small animals. CFIR uses three-dimensional volumetric image guidance for localization and targeting of the radiation dose, minimizes radiation exposure to non-targeted brain regions, and allows for conformal dose distribution with sharp beam boundaries. This protocol allows one to ask questions regarding the function of adult-born neurons, but also opens areas to questions in areas of radiobiology, tumor biology, and immunology. These radiological tools will facilitate the translation of discoveries at the bench to the bedside.

Introduction

Recent discoveries have demonstrated that the adult mammalian brain can undergo a remarkable degree of plasticity. Adult-born neurons are generated throughout adulthood in specialized niches of the mammalian brain¹. What is the function of these adult-born neurons? And more so, do they play a role in physiology and behavior? Studies on this topic have traditionally focused on the subventricular zone of the lateral ventricles and the subgranular zone of the hippocampus; however, recent studies have characterized neurogenesis in other brain regions such as the mammalian hypothalamus². Neurogenesis has been reported in the postnatal and adult hypothalamus²⁻¹⁰, and the function of these newborn hypothalamic neurons remains an active area of investigation.

The functional characterization of adult-born neurons remains a significant challenge for the neuroscience field in general. Selective inhibition of specific neural progenitor populations remains limited by the lack of available molecular markers that are unique to single neural progenitor populations¹¹. Thus, selective deletion of adult-born neurons from these neural progenitors via genetic targeting remains difficult. Likewise, viral delivery to target adult-born neurons suffers from potential confounding variables such as introducing injury and inflammation into the environment¹².

New radiological tools are emerging, however, that allow one to circumvent these confounds and investigate these questions through accurate and precise anatomical targeting in small animals. Ionizing radiation inhibits the birth and differentiation of new neurons, and allows a non-invasive method to target neural progenitor populations¹³⁻¹⁵. Recently, we described a germinal region of the mammalian hypothalamic median eminence (ME) that we termed the hypothalamic proliferative zone (HPZ)². We found that when young adult female mice were given a high-fat diet (HFD), levels of neurogenesis in HFD-fed mice were substantially higher than their normal chow (NC) fed controls in this ME region². To test whether adult neurogenesis within the hypothalamic ME regulates metabolism and weight, we sought to disrupt this process. The median eminence is a small unilateral structure at the base of the third ventricle from which regulatory hormones are released. In order to inhibit proliferation and subsequent neurogenesis without altering the other physiological functions of this brain region, we developed a non-invasive focal irradiation technique to selectively inhibit the birth of newly born adult neurons in the hypothalamic median eminence².

A number of groups have employed radiation to suppress neurogenesis in canonical regions¹⁴⁻²⁸. However, previous radiological approaches have generally targeted large areas, or often unintentionally also targeted multiple brain areas where neurogenesis has been reported, making it difficult to unambiguously associate any behavioral defects observed with defects in specific neural progenitor populations. The capability for more targeted irradiation is provided by radiological platforms that combine computer tomography-guided imaging with focal beam irradiation (CFIR) delivery to enable precise anatomical targeting²⁹⁻³⁶. Radiation beams as small as 0.5 mm in diameter are available to target specific neural progenitor populations³⁵. This methodology allows us to target the hypothalamic ME and arrest proliferation and block neurogenesis in small animals. Following radiological treatment on these progenitor populations, physiological and behavioral tests can be performed to illuminate the potential function of adult-

born cells. Focal targeting is especially important for our application since the pituitary gland is located close to the hypothalamic median eminence; irradiation of the pituitary may affect hormonal function and subsequently confound results.

The biological basis for the suppression of neurogenesis following irradiation still remains unclear. Previous radiation studies have relied on large area beams, and have concluded that the suppression of neurogenesis is mediated through an inflammatory response^{14, 37}. As such it is unclear whether highly focal irradiation could suppress neurogenesis, since it does not evoke a substantial inflammatory response. However, recent studies by our group of the classic neurogenic region in the hippocampus have demonstrated that highly focal irradiation with a dose of 10 Gy can suppress neurogenesis for at least 4 weeks after irradiation³⁵.

To interrogate the function of adult-born hypothalamic neurons in the median eminence, we use a precision radiation device capable of delivering CT imaging in combination with small-diameter radiation beams to inhibit ME neurogenesis. Using an X-ray tube attached to a gantry that rotates over a range of 360°, we deliver arc-beam micro irradiation beam with the use of a robotically controlled specimen stage that allows rotation of an animal subject during radiation treatment (**Figure. 1**). A high-resolution, X-ray detector is used to acquire images when the gantry is in the horizontal position³³. For this study, CT images were reconstructed with an isotropic voxel size of 0.20 mm. On-board CT imaging allowed the identification of a target while the animal is in the treatment position. The target was localized using the CT navigation dose-planning software, which was included with our commercially available radiological platform. After localizing our ROI by CT imaging, the animal was moved to the appropriate treatment position by the robotic specimen stage which has four degrees of freedom (X, Y, Z, θ). Through a combination of gantry and robot stage angles, beams can be delivered from nearly any direction relative to the animal, and stereotactic arc-like treatments are possible²⁹. For these and all other imaging studies, the mice were positioned in an immobilization device that allows delivery of anesthetic isoflurane gas while restricting movement. The immobilization bed is CT compatible, and connects to the robotic specimen stage³⁴.

We expect that CFIR will provide conceptual advances in a number of research areas. Although we use radiological targeting of the hypothalamic median eminence as proof of principle of this technique, CFIR can be used to target any region of the body of any small model organism in principle. In the neurosciences, for example, we envision this technique could be used to evaluate the function of actively proliferative progenitor populations that have suggested to exist in other circumventricular organs, such as the area postrema^{38, 39}, subfornical organ⁴⁰, and the pituitary⁴¹. Longstanding controversies regarding the functional role of adult neurogenesis and identifying a causal role in behavior can also now be better addressed. In songbird, this technique might address the role of adult neurogenesis in maintaining the robust and seasonal behavior of birdsong⁴², which have been hampered by the ability to selectively inhibit neurogenesis in specific brain regions. Understanding this robust behavioral model might shed new insight into the role of adult neurogenesis in regulating other sexually dimorphic behaviors. Alternatively, in the metabolic field, CFIR might be used to explore aspects of the role of hepatocyte proliferation and its role in metabolism and energy balance. The possibility for conceptual advance in multiple research disciplines is enhanced by the introduction of this technique.

In this paper, we demonstrate the capabilities of CFIR for precision anatomical targeting of a focal irradiation beam. Although we initially developed this small animal radiation research platform (SARRP) for our studies, other similar devices are now commercially available that can accomplish similar CT-guided focal irradiation^{43, 44}. Hence, we generalize this CFIR protocol with steps required for all research platforms rather than those specific for SARRP. The advantages of CFIR over previous radiological approaches to inhibit neurogenesis is that this technique allows three-dimensional volumetric image guidance for localization and targeting of the dose, conformal dose minimizes exposure to non-targeted brain regions, and high precision beam geometry allows for conformal dose distribution with sharp beam boundaries. We outline how to use CT-guided imaging to target the dose to a specific anatomical region, and upon doing so, how to visualize the radiation dose distribution directly in tissue using immunohistochemical staining for γ -H2AX, a marker of DNA double-stranded breaks^{35, 45-48}. The use of this approach for selective irradiation of neurogenic niches may have significant implications in revealing the functional role of new adult-born neurons on physiology and disease.

Protocol

Animal Usage

Obtain approval from institutional Animal Care and Use Committee for standard care and use protocols. The current protocol was developed for focal irradiation studies on 5.5-10 week-old adult C57BL6/J mice, as previously described (**Figure 2**)². However, other ages and small animal species (rats, hamsters, ground squirrels, etc) can also be used, provided that effective anesthesia protocols and a radiographic reference atlas allowing identification of the region of interest (ROI) are available.

1. Calibration of CT-guided radiological platform

Perform film-based calibrations for radiation dose on the radiological platform in advance for each collimator size and type of X-ray tube filter used. In order to target an arc beam of irradiation at the desired target site, use the radiation dose-planning software⁴⁹ available on most commercial radiation platforms to calculate required delivery time based on the radiation dose, the depth of the region of interest (ROI) based on CT scans of the mouse, and the rotation speed of the robotic platform; details on this are left out of this protocol as they differ between radiation platforms. **For the purposes of visualizing the ventrobasal hypothalamus² (Figure 3) with CT imaging, operate the X-ray tube with a 0.4-mm focal spot and beam energy of 100 kVp with 1 mm Al filtration. For focal irradiation of the HPZ, operate the X-ray tube at 225 kVp, 13 mA, and a 1-mm focal spot with filtration of 0.15 mm Cu, to deliver 10Gy of radiation at a tissue depth of 0.6 cm over a treatment time of 4.6 minutes.** Targeting between different ROIs will require calculating different parameters.

1.1 If studying the effects of high-fat diet on neurogenesis in the median eminence as previously described², obtain four-week old female C57BL6/J mice from Jackson Mouse laboratories, and house four mice per cage. Switch food from normal chow to a high-fat diet at five weeks old. Allow mice to acclimate to new housing and food. Perform CFIR treatment at 5.5 weeks old. Transport subjects to the operation room that contains the radiological platform.

Minimize stress levels during transfer. Prepare isoflurane gas anesthesia chamber. Then, add a single mouse into chamber. In parallel, prepare heating pad (low setting) for post-treatment.

1.2 Once mouse is under and no longer responding to foot-pad compression, bring the subject to the radiological platform and place on the immobilization bed of the robotic stage. Place subject's mouth into the nose-cone anesthesia cup, and teeth into the bite guard (**Figure 1D**). Lay mouse flat on the immobilization bed and check to see if it continues to maintain unresponsiveness. If so, tape down mouse to the bed with gauze tape. While taping down the mouse to the bed, make sure the head is leveled to a horizontal plane. This can be determined by pulling up the ears and seeing if they are leveled. Once the mouse is in the correct position, close the lead protective shield.

1.3 Acquire the computer-tomography scan using on-board software of the experimenter's radiological platform (this will differ between platforms), which will provide a three-dimensional anatomical structural scan of the mouse subject. Check to see if the mouse head is level to the horizontal plane. If not, repeat steps 2-3 until the subject's head is leveled.

1.4 Identify ROI by CT image. Calculate distance from ROI to the surface of the skull using a 45 degree angle to the horizontal plane as shown in **Figure 3E**.

1.5 Using on-board software, take an X-ray of the mouse subject from above as shown in **Figure 4A**. Then, remove mouse from the radiological platform, put on heating pad, and monitor until active.

1.6 From the coronal CT images, calculate the average ROI anatomical depth of at least three mice in order to determine delivery dosing. As an example from a previous study² where 10Gy of irradiation was administered to the ventrobasal hypothalamus, the depth of the ROI from the skull (from a 45 degree angle) is 0.66cm (See **Figure 3E**). Knowing that, the researchers used the dose planning software (DPS) installed on their radiological platform to calculate the appropriate rotation speed and length of treatment to achieve desired dosage to the ROI.

1.7 After determining treatment duration and rotation speed of the robotic stage with the dose-planning software, measure dose distributions of the calculated parameters with GAFchromic radiation-sensitive films embedded in a water-equivalent plastic mock-mouse model. To do this, embed three GAFchromic radiation-sensitive films between four vertically stacked water-equivalent plastic blocks²⁹ as shown in **Figure 4B**.

1.8 Place mock mouse model containing GAFchromic films on robotic stage, and run the focal irradiation beam with the newly calculated parameters. For example, to target the ventrobasal hypothalamus, input the parameters of 0.15mm Cu filter, 225kVp, 13 mA, 1-mm diameter radiation beam setting, 45 degree gantry angle, 1.3 degree/sec rotation, and 4.6 minutes to achieve an ROI radiological dose of 10Gy.

1.9 Following irradiation, check films for pattern and intensity of radiation dosage. For a 360 degree angle rotation with the parameters listed to target the ventrobasal hypothalamus, a dark ring in the film above the isocenter, a small crisp spot at the isocenter film, and a lighter ring in the film below the isocenter corresponding to the cone-beam administration of the irradiation will be observed (**Figure 4B**).

1.10 Superimpose isocenter GAFchromic film over the X-rays of mouse subjects where the parameters were calculated from. The irradiated focal point at isocenter should overlap with the desired ROI region as shown in **Figure 4C**.

Alternative method: If difficulty in targeting brain ROI persists, use iodine contrast injected intrathecally to enhance visualization of ventricles under CT images. For the sake of brevity, this procedure is left out of this protocol, but is previously described^{35, 50}. Iodine contrast will provide additional ventricular landmarks (**Figure 5A**).

2. Determining Accuracy of Irradiation Beam

Further confirm CFIR beam accuracy by direct visualization of the radiation beam in tissue^{2, 35, 51}. To do this, perform immunohistochemistry to detect γ H2AX⁵¹, a histone protein and an early marker of DNA double strand breaks. Mouse subjects must be transcardially perfused and fixed within one hour of irradiation. Following irradiation, DNA repair rapidly ensues, and levels of γ H2Ax decrease significantly³⁵.

2.1 Repeat steps 1.1-1.3.

2.2 After the target is identified on CT, the mouse subject is moved under robotic control to align this target with the radiation delivery beam. Input calculated parameters (rotation speed and length of treatment to achieve desired dosage) from step 1.6 into dose-planning software and begin treatment. Treatment is delivered with the gantry pointed to 45 degrees from the vertical while the mouse rotates about a vertically-oriented axis.

2.3 Following irradiation, perform transcardial perfusion on mouse subjects. Perform perfusion within one hour⁵². Following perfusion, immersion fix brains in 4% PFA/PBS and gently rock overnight at 4°C.

2.4 The following morning, wash 3x5 minutes in PBS to remove paraformaldehyde fixative. Then, immerse in 30% sucrose in 1xPBS on a rocker at 4°C.

2.5 Gently rock at 4°C (usually 12-16 hours), until brain sinks to bottom of tube. This serves as a cryoprotection step. Once brains sink, remove brain with a perforated spoon to prevent excess 30% sucrose/1xPBS transfer. Quickly embed in freezing medium on dry ice. Swirl freezing medium with pipette tip and align brain in plastic mold.

2.6 Once completely frozen, transfer brain blocks to -20C freezer for storage.

2.7 On the day when immunohistochemistry will be performed, section coronally at 40um thickness, and float into a 24-well plate containing PBS with a thin paintbrush. Sections should be kept in correct serial order for immunostaining to determine irradiation coverage of target region.

2.8 Pre-warm 0.01M sodium citrate solution to 80°C in water bath in preparation for antigen retrieval step. Simultaneously, while the sodium citrate is warming, perform three 5-minute washes in 0.01M PBS.

- 2.9 Once sodium citrate solution is at 80°C, submerge brain sections in the sodium citrate buffer solution. Leave in water bath at 80°C for 1 hour.
- 2.10 Remove section and allow sodium citrate solution to reach room temperature, then perform three 5-minute washes in 0.01M PBS.
- 2.11 Block brain sections for one-hour in PBS-Triton containing 5% normal goat serum.
- 2.12 Incubate brain sections overnight in PBS-Triton containing 5% normal goat serum with 1:700 concentration of Ms anti-phospho-H2AX primary antibody at 4°C.
- 2.13 The next day, perform three 15-minute washes in 0.01M PBS-Triton.
- 2.14 Incubate brain sections PBS-Triton containing 5% normal goat serum with goat anti-mouse secondary antibody conjugated with 488nm fluorophore at 1:500 concentration for 2 hours.
- 2.15 Perform three 15-minute washes in 0.01M PBS-Triton.
- 2.16 Perform 4',6-diamidino-2-phenylindole (DAPI) stain (1:5000 in PBS) for 10 minutes to visualize nucleus. Then, wash brain sections for 5 minutes with PBS.
- 2.17 Mount on electrostatically charged microscope slides by floating section in PBS. Wipe off excess PBS and allow slides to dry. Coverslip the slides using mounting medium and allow the slides to dry in the dark at room temperature overnight.
- 2.18 Take pictures of serial coronal sections with fluorescent microscope. γ H2Ax immunostaining (green) indicates site of irradiation. DAPI (blue) is a nuclear stain (**Figure 5B**).

3 Preparation of Mouse Subjects for Focal Irradiation

Examine γ H2Ax immunostaining results. Once satisfied with the calibration and targeting of the irradiation beam, proceed with the experiment. At this point, the total time required to treat a mouse (from animal setup to completion of beam delivery) is approximately 10-15 minutes for a 10-Gy treatment with a 1-mm beam.

3.1 Order four-week old C57BL6/J female mice from Jackson Mouse laboratories. House four mice per cage, and switch food from normal chow to a high-fat diet at five weeks old. Ear punch mice to give them unique identifying marks. Monitor health of mice daily. Note: metallic markers cannot be used as they will result in streaking artifacts on the CT.

3.2 Weigh mice the day before radiation or sham treatment. Split mice into two cohorts for radiation or sham treatment and ensure that there is no significant difference in weight between cohorts. On the day of treatment, when mice are six weeks old, re-weigh all mice and record their mass. Gently transport both cohorts to the radiological platform. Take care to minimize stress levels.

3.3 Prepare isoflurane gas anesthesia chamber. Anesthetize two mice, one in the pre-determined irradiation group, and another in the sham control group. Prepare heating pad set in the low setting for post-operative treatment.

3.4 Follow steps 1.2-1.4 for the mouse to receive irradiation. For the sham mouse, keep mouse in anesthesia chamber while treatment is going on. Make sure that anesthesia chamber is near the CFIR platform so any effects on ambient radiation are factored in. After the target is identified on CT, move mouse subject under robotic control to align this target with the radiation delivery beam. Input calculated parameters (rotation speed and length of treatment) into dose-planning software.

3.5 Once irradiation treatment is complete, return both sham and irradiated mice to heating pad, and monitor until they wake up.

3.6 Return both sham and irradiated mice to animal facility. Monitor every day. Weigh the mice every half week. To confirm irradiation of targeted hypothalamic proliferative zone, administer intraperitoneal injections of BrdU (50mg/kg) three days post treatment and examine neurogenesis between groups by co-labeling of immunohistochemistry for BrdU and a neuronal marker one month following initial BrdU exposure (**Figure 6**)².

Representative Results

Assessing CT-guided Targeting and Accuracy

The mechanical calibration of the system is critical to ensuring that beams from various angles all intersect in a single point. Calibration was accomplished with a semi-automatic imaging-based method, where end-to-end alignment accuracy has been measured to be 0.2 mm²⁹. This accuracy is highly critical as the volume of the hypothalamic median eminence structure is small². To test this calibration, we measured dose distributions with GAFchromic radiation-sensitive films embedded in a water-equivalent plastic mock-mouse model³⁵ (**Figure 4B**). Briefly, a CT-scan of the mouse subject was taken, and our ventrobasal hypothalamic target site was identified. Delivery and rotation speed were calculated, and the appropriate collimator and filtration were attached to ensure 10Gy of radiation was delivered. A mock-mouse model designed from a water-equivalent plastic structure embedded with GAFchromic radiation-sensitive films was then substituted for the real mouse subject to measure dose distribution at different focal planes. **Figure 4B** shows end-to-end test results from an arc treatment with the 1-mm-diameter beam using GAFchromic films in a mock-mouse platform. The gantry was set at a 45° angle with respect to the mock mouse model while the robotic specimen stage was rotated around a vertically oriented axis, generating an “arc” or cone of radiation. The full width at half maximum (FWHM) is 2.31 mm, which is larger than 1.0 mm since the arcs impinge on the film at an angle. Theoretically the beam size at this angle should be 2.0 mm. The focal beam spot shown in **Figure 4** demonstrates the precision alignment of beams from different directions. This film can be overlaid on top of the real mouse subject, demonstrating beam position and precision (**Figure 4C**).

Using a 1 mm diameter beam collimator, an arc technique was used to deliver 10 Gy to the target point in our mouse subject. Previous measurements²⁹ indicate that this technique provides very low doses of radiation (<0.1 Gy) outside the 1 mm target. The area of the pituitary gland and surrounding structures is therefore effectively shielded from focal irradiation of the ventrobasal hypothalamus. The accuracy of the beam targeting has been measured in previous studies to be within 0.2 mm both in phantom tests²⁹ and tissue sections³⁵.

While not required, CT-guided targeting of the ROI can be enhanced by an injected intrathecal iodine contrast to enhance CT-guided targeting for our brain application (**Figure 5A**). As this is an invasive and cumbersome procedure, this contrast is not used often, and not described in this protocol. Details for this protocol can be found in Ford *et al.*, 2011 and Chaichana *et al.*, 2007. The advantages of this iodinated contrast are that the lateral and third ventricles are clearly visualized in CT scans acquired on a CFIR radiological platform (**Figure 5A**). The target was the median eminence, at the base of the third ventricle, and was identified using CT-guided navigation software and automatically imported into the robot positioning interface. Bony cranial structures were identified and used as anatomical landmarks for subsequent studies where iodine contrast was not employed.

Beam Targeting Validation with γ -H2AX

To further confirm our CT-guided targeting of the hypothalamic ME, we visualized the 1-mm irradiation beam in tissue by indirect examination of double-stranded DNA breaks that arises following irradiation. H2AX histone protein is phosphorylated after DNA double-strand breaks. γ -H2AX has been widely used in brain and other tissues⁴⁶⁻⁴⁸, and the number of γ -H2AX⁺ foci appears to correlate well with radiation dose over a wide range of doses^{51, 53}. We observed clear visualization of the beam following γ -H2AX immunostaining (**Figure 5B**). Resultant γ -H2AX staining showed precise targeting of the expected location. The beam edge was also extremely sharp, in agreement with film-based physics commissioning measurements that indicate a 20–80% penumbra of 0.3 mm⁵⁴. We previously measured the distance between the intended target and the center of the beam as visualized in the tissue sections³⁵. The center of the beam was offset from the intended target by a mean distance of 0.19 ± 0.36 mm (standard deviation) in 10 irradiated mice after factoring for effects of tissue shrinkage during fixation and processing³⁵.

Using a stereotactic-like arc treatment consisting of an arc at 45° from the vertical, we show we were able to effectively target the ventrobasal hypothalamus, without irradiating other neurogenic niches (**Figure 5C-D**). Irradiation of surrounding areas was minimal, and there was a boundary in radiation exposure as demonstrated by GAF-chromic film (**Figure 4B**) and γ -H2AX immunostaining (**Figure 5B-D**). The tissue dorsal to the hypothalamic ME shows light γ H2AX staining (**Figure 5B**) since the radiation beams enter through this region and also possibly because of enhancement by the overlaying bone even though a relatively hard X-ray beam was used (225 kVp, 0.15 mm Cu filtration).

Effects on Neurogenesis

Upon confirming the specificity of our CT-guided irradiation delivery, we examined the effect of 10Gy of irradiation on levels of ME neurogenesis. Adult mice were fed a high-fat diet, received

the radiation or sham treatment, and then subsequently BrdU injections as previously described beginning at 6 weeks old². Mice were sacrificed for examination at 10 weeks old, one month after the first BrdU injection. Irradiated HFD-fed adult mice exhibited ~85% inhibition of ME neurogenesis compared with sham-treated controls (**Figure 6A**)². The arcuate nucleus, an adjacent structure bordering the irradiation site, was examined for changes in neurogenesis, and found to have no statistically significant difference between irradiated animals and sham controls (**Figure 6A**)².

Function of Adult-born Median Eminence Hypothalamic Neurons

Changes in irradiated and sham mice were examined following treatment. Fur coat and response to touch appeared normal. A chemistry panel and complete blood count panel was examined one week following irradiation treatment, and no significant difference was observed (n=9/group). In high-fat fed mice where we observed a ~85% reduction in adult-born ME neurons one month following irradiation (**Figure 6A**), irradiated mice had decreased weight gain over time compared to the sham treated group (**Figure 6C**). In contrast, normal-chow fed control mice, where observed levels of ME neurogenesis were significantly lower than their high-fat fed counterparts², did not have a statistically significant difference in weight between sham versus irradiated groups (**Figure 6B**). Interestingly, this reduced weight gain in irradiated high-fat fed mice is accompanied by changes in metabolism and activity as previously described in detail by our group² (**Figure 6D-I**).

Figure Legends

Figure 1: Computer tomography-guided focal irradiation (CFIR) platform

(A) CFIR utilizes a precision radiation device capable of delivering CT-guided irradiation with small beams. An example of one CFIR platform is the small animal radiation research platform (SARRP). With lead shielding (as shown), the SARRP stands at 81 inches (height) by 58 inches (width) by and 41 inches (depth) at 5170 pounds. (B) Using a dual source X-ray tube attached to a gantry that rotates 360°, the SARRP uses a robotically control specimen stage that allows rotation of an animal subject throughout radiation treatment. (C) CFIR hardware is composed of an X-ray source, collimator, rotating gantry, animal support, rotating robotic specimen stage, and electronic imager. (D) The mouse subject is placed in an immobilization bed with gas anesthesia input on the robotic specimen stage. From Armour *et al.*, 2010. (E) CFIR hardware should include customizable collimating cones for focal irradiation delivery of different sizes.

Figure 2: Experimental Paradigm

Female C57Bl/6 mice were ordered from Jackson mouse laboratories, and acclimated to resident cages at four weeks old. Mouse subject were switched to an *ad libitum* high-fat diet at five weeks old, and split into two treatment groups: the irradiated or sham cohorts. Physiological assessments were taken longitudinally prior and following treatment. Irradiation or sham treatments were administered at 5.5 weeks. Intraperitoneal BrdU injections were given at six weeks old as previously described².

Figure 3: Region of Interest Localization

The hypothalamic proliferative zone (HPZ), a neurogenic region located in the hypothalamic median eminence, is located in the ventral mediobasal hypothalamus. (A) The HPZ region of interest (ROI) is highlighted by red cross-hairs in a 3-D Nissl reference atlas volume from the Allen Brain Atlas Data Portal (Position: 7.041, 7.211, 5.564) (Available from <http://mouse.brain-map.org/>)⁵⁵. (B) Coronal brain section of the ROI in nineteen day old mice. BrdU immunohistochemistry (green) reveals that the ROI (white arrowhead) contains proliferative cells. The density of proliferative cells in the HPZ is restricted in the anterior to posterior axis, with density highest at -1.75mm Bregma. Tissue sections are counter-stained with DAPI nuclear marker (blue). Figure from Lee *et al.*, 2012a. (C-E) CT-imaging on a CFIR platform allows targeting the HPZ ROI (red cross-hairs) by arc beam radiation delivery. CT-image of mouse subject in the horizontal plane (C), sagittal plane (D), and coronal plane (E). (E) Distance from the surface of the skull to the ROI is 0.62 cm (red line). Scale bars = 1mm (A), 50 μ m (B), and 0.62cm (C-E).

Figure 4: Calibration of Irradiation Delivery

(A) X-ray of a mouse subject secured in the immobilization device on the SARRP robotic stage. (B) Calculated ROI coordinates are inputted and targeted against a mock mouse model. The phantom model is composed of GAFchromic radiation-sensitive films embedded in a water-equivalent plastic. Films located above, at, and under the ROI isocenter detect the dose distribution. A 45 degree arc radiation beam from the SARRP delivers a cone-shaped dose distribution to the ROI, and converges at the isocenter (penumbra spot). (C) Superimposition of dosimetry-film acquired with 1-mm radiation beam in phantom with an X-ray of a real mouse subject (yellow line). White circle (arrow) indicates 10-Gy radiation dose focally targeted to HPZ. Dotted line outlines brain. Panel from Lee *et al.*, 2012a.

Figure 5: Confirmation of Radiation Delivery

CT imaging with iodine contrast can enhance visualization of the ROI if normal CT imaging does not suffice. (A) Mouse subjects received iodine contrasts as previously described (Panel from Lee *et al.*, 2012). CT images in the coronal, horizontal, and sagittal plane are shown from left to right. (B) Confirmation of radiation delivery of in tissue can be detected by immunohistochemistry for γ H2AX, a marker of DNA double-stranded breaks. γ H2AX immunostaining shows radiation beam delivery targeted to the ROI HPZ in the ventral mediobasal hypothalamus. γ H2AX immunostaining is not observed in the subventricular zone of the lateral ventricles (C), or the subgranular zone of the hippocampus (D) of the same mouse subject. (B-D) Sections are counterstained with DAPI (From Lee *et al.*, 2012a).

Figure 6: Focal inhibition of ME neurogenesis results in alterations in weight and metabolism.

(A) The median eminence (ME) located in the ventral mediobasal hypothalamus was targeted for irradiation. The arcuate nucleus (ArcN) is the neighboring anatomical structure. One month following treatment, the percentage of BrdU⁺ Hu neurons from sham versus irradiated cohorts were quantified by immunohistochemistry in the ME and ArcN. Levels of ME neurogenesis were significantly reduced in irradiated versus sham cohorts (n=5/cohort, *** = $p < 0.0001$). Levels of ArcN neurogenesis were not affected (n=3/cohort, n.s. = not significant). (B) Normal chow fed (NC) and (C) high-fat fed (HFD) mice were examined longitudinally for alterations in

weight following irradiation or sham treatment (**B**, n=12/cohort; **C**, n=9/cohort) (**D-E**) One month following treatment, irradiated and sham treated HFD-fed mice were examined by quantitative magnetic resonance spectroscopy for analysis of % fat mass and % lean mass. Irradiated mice had significantly less % fat mass and significantly more % lean mass than sham controls (n=5, * = p<0.05). Total mass: (Sham) 21.0±0.3g, (Irradiated) 18.86±0.4g; Lean mass: (Sham) 14.6±0.2g, (Irradiated) 13.9g±0.3g; Fat Mass: (Sham) 3.9±0.2g, (Irradiated) 2.6±0.3g (n=5, * = p<0.05). (**F-I**) Irradiated and sham treated adult mice were placed in a Comprehensive Lab Animal Monitoring System (CLAMS) for simultaneous measurements of food intake, physical activity, and whole-body metabolic profiling two weeks after treatment. Following acclimation in the testing chamber, irradiated mice were observed to have significantly greater energy expenditure, total activity, and VO₂ (ml/kg/hr) compared to sham controls during the dark portion of the day (n=11,12; * = p<0.05). (**G**) No significant difference was observed in the respiratory exchange rate (RER) (n=11,12). Subfigure **A** is generated from data previously published in Lee *et al.*, 2012a and Lee *et al.*, 2012b. Subfigures **C-I** from Lee *et al.*, 2012a.

Discussion

CT-guided focal irradiation (CFIR) is a novel and complete system approach capable of delivering radiation fields to targets in small animals under robotic control using CT-guidance³². The capability of CFIR to deliver highly focused beams to small animal models provides new research opportunities to bridge laboratory research and clinical translation. This paper describes the CFIR approach for precise radiation delivery to specifically target a hypothalamic neural progenitor population. We demonstrate here how to calibrate and confirm radiation delivery specificity via X-ray film and in brain tissue by immunohistochemistry.

In addition, we show how this technique can be used to inhibit neurogenesis in a specific brain region. We demonstrate that we are able to target the ventrobasal hypothalamus, and inhibit neurogenesis in the median eminence, without altering levels of neurogenesis in adjacent structures. Inhibition of ME neurogenesis is accompanied by changes in metabolism and activity, as well as reduced weight gain on a high-fat diet in irradiated versus sham treatment groups (**Figure 6**)². These data suggests a role for these adult-born hypothalamic neurons in regulating metabolism and energy homeostasis. Moreover, it suggests that an excess high-fat diet can alter critical metabolic circuitry even in adulthood³. Our results represent an important expansion on the known function of adult-born neurons, and sheds light on a new hypothalamic neural progenitor population³. Potential caveats to this approach are that irradiation inhibits progenitor proliferation rather than neurogenesis per se and thus is also possible that physiological changes post-treatment may be partially accounted for by disruption of other adult cell genesis. Future steps will include the development of genetic tools to inhibit the proliferation of this specific neural progenitor population, which will provide substantial clarity to the functional role these progenitors and their progeny play in the regulation of physiology³.

Taken together, however, this radiological platform serves as an important starting point in performing medium throughput screens on neural progenitors and their progeny. This

radiological technique is not limited to research questions in the neurosciences, however, and we expect CFIR to expand the conceptual advance in a number of research disciplines. The recent availability of commercially-sold CT-guided radiological platforms provides an opportunity for researchers to use these capabilities of this platform for their research questions (**Figure 1**). Several alternatives are commercially available that allow one to perform image-guided small animal irradiation. Furthermore, CT-guided focal irradiation systems can also be built in house, as was the case with the system used for these studies at Johns Hopkins^{29-33, 35}.

Performing this degree of focal targeting requires proper calibration and targeting of the ROI. While this technique will initially take training in order to become familiar with the CFIR platform and its dose-planning software, operation of the device is rather easy after understanding the protocol and capabilities of the platform. It is recommended that the operator practices calibrating the radiation beam several times prior to running full-scale longitudinal experiment. That said, once fluent in the operation of CFIR, research studies should move quickly.

This CFIR protocol described herein uses three-dimensional volumetric image guidance for localization and targeting of the dose, conformal dose minimizes exposure to non-targeted brain regions, and high precision beam geometry allows for conformal dose distribution with sharp beam boundaries. This allows one to ask questions regarding the function of adult-born neurons, but also opens areas to questions to the role of cell proliferation in areas such as physiology, tumor biology, and immunology. This method can be expanded in several ways with contrast dyes and bioluminescence to enhance visualization^{35, 56}. Efforts are now underway to enhance CFIR hardware capabilities further, and the platform is now being modified to include an on board positron emission tomography scanner⁵⁶. These will facilitate the expansion of tools available to researchers and aid in translating discoveries at the bench to the bedside.

Acknowledgments

We thank C. Montojo, J. Reyes, and M. Armour for technical advice and assistance. This work was supported by US National Institutes of Health grant F31 NS063550 (to D.A.L.), a Basil O'Connor Starter Scholar Award and grants from the Klingenstein Fund and NARSAD (to S.B.). S.B. is a W.M. Keck Distinguished Young Scholar in Medical Research.

Disclosure

J.W. has a research funding and consultation agreements with Xstrahl, Inc.

References

1. Ming, G.L. & Song, H. Adult neurogenesis in the mammalian brain: significant answers and significant questions. *Neuron* **70**, 687-702 (2011).
2. Lee, D.A. et al. Tanycytes of the hypothalamic median eminence form a diet-responsive neurogenic niche. *Nat Neurosci* **15**, 700-2 (2012).

3. Lee, D.A. & Blackshaw, S. Functional implications of hypothalamic neurogenesis in the adult mammalian brain. *Int J Dev Neurosci* (2012).
4. Pencea, V., Bingaman, K.D., Wiegand, S.J. & Luskin, M.B. Infusion of brain-derived neurotrophic factor into the lateral ventricle of the adult rat leads to new neurons in the parenchyma of the striatum, septum, thalamus, and hypothalamus. *J Neurosci* **21**, 6706-17 (2001).
5. Kokoeva, M.V., Yin, H. & Flier, J.S. Neurogenesis in the hypothalamus of adult mice: potential role in energy balance. *Science* **310**, 679-83 (2005).
6. Pierce, A.A. & Xu, A.W. De novo neurogenesis in adult hypothalamus as a compensatory mechanism to regulate energy balance. *J Neurosci* **30**, 723-30 (2010).
7. Ahmed, E.I. et al. Pubertal hormones modulate the addition of new cells to sexually dimorphic brain regions. *Nat Neurosci* **11**, 995-7 (2008).
8. Xu, Y. et al. Neurogenesis in the ependymal layer of the adult rat 3rd ventricle. *Exp Neurol* **192**, 251-64 (2005).
9. Kokoeva, M.V., Yin, H. & Flier, J.S. Evidence for constitutive neural cell proliferation in the adult murine hypothalamus. *J Comp Neurol* **505**, 209-20 (2007).
10. Perez-Martin, M. et al. IGF-I stimulates neurogenesis in the hypothalamus of adult rats. *Eur J Neurosci* **31**, 1533-48 (2010).
11. Shimogori, T. et al. A genomic atlas of mouse hypothalamic development. *Nat Neurosci* **13**, 767-75 (2010).
12. Ming, G.L. & Song, H. Adult neurogenesis in the mammalian central nervous system. *Annu Rev Neurosci* **28**, 223-50 (2005).
13. Limoli, C.L. et al. Radiation response of neural precursor cells: linking cellular sensitivity to cell cycle checkpoints, apoptosis and oxidative stress. *Radiat Res* **161**, 17-27 (2004).
14. Monje, M.L., Mizumatsu, S., Fike, J.R. & Palmer, T.D. Irradiation induces neural precursor-cell dysfunction. *Nat Med* **8**, 955-62 (2002).
15. Wojtowicz, J.M. Irradiation as an experimental tool in studies of adult neurogenesis. *Hippocampus* **16**, 261-6 (2006).
16. Mizumatsu, S. et al. Extreme sensitivity of adult neurogenesis to low doses of X-irradiation. *Cancer Res* **63**, 4021-7 (2003).
17. Snyder, J.S., Hong, N.S., McDonald, R.J. & Wojtowicz, J.M. A role for adult neurogenesis in spatial long-term memory. *Neuroscience* **130**, 843-52 (2005).
18. Santarelli, L. et al. Requirement of hippocampal neurogenesis for the behavioral effects of antidepressants. *Science* **301**, 805-9 (2003).
19. Saxe, M.D. et al. Ablation of hippocampal neurogenesis impairs contextual fear conditioning and synaptic plasticity in the dentate gyrus. *Proc Natl Acad Sci U S A* **103**, 17501-6 (2006).
20. Duan, W. et al. Sertraline slows disease progression and increases neurogenesis in N171-82Q mouse model of Huntington's disease. *Neurobiol Dis* **30**, 312-22 (2008).
21. Rola, R. et al. Radiation-induced impairment of hippocampal neurogenesis is associated with cognitive deficits in young mice. *Exp Neurol* **188**, 316-30 (2004).
22. Hellstrom, N.A., Bjork-Eriksson, T., Blomgren, K. & Kuhn, H.G. Differential recovery of neural stem cells in the subventricular zone and dentate gyrus after ionizing radiation. *Stem Cells* **27**, 634-41 (2009).

- 682 23. McGinn, M.J., Sun, D. & Colello, R.J. Utilizing X-irradiation to selectively eliminate
683 neural stem/progenitor cells from neurogenic regions of the mammalian brain. *J Neurosci*
684 *Methods* **170**, 9-15 (2008).
- 685 24. Panagiotakos, G. et al. Long-term impact of radiation on the stem cell and
686 oligodendrocyte precursors in the brain. *PLoS One* **2**, e588 (2007).
- 687 25. Shinohara, C., Gobbel, G.T., Lamborn, K.R., Tada, E. & Fike, J.R. Apoptosis in the
688 subependyma of young adult rats after single and fractionated doses of X-rays. *Cancer*
689 *Res* **57**, 2694-702 (1997).
- 690 26. Tada, E., Parent, J.M., Lowenstein, D.H. & Fike, J.R. X-irradiation causes a prolonged
691 reduction in cell proliferation in the dentate gyrus of adult rats. *Neuroscience* **99**, 33-41
692 (2000).
- 693 27. Tada, E., Yang, C., Gobbel, G.T., Lamborn, K.R. & Fike, J.R. Long-term impairment of
694 subependymal repopulation following damage by ionizing irradiation. *Exp Neurol* **160**,
695 66-77 (1999).
- 696 28. Hopewell, J.W. & Cavanagh, J.B. Effects of X irradiation on the mitotic activity of the
697 subependymal plate of rats. *Br J Radiol* **45**, 461-5 (1972).
- 698 29. Matinfar, M., Ford, E., Iordachita, I., Wong, J. & Kazanzides, P. Image-guided small
699 animal radiation research platform: calibration of treatment beam alignment. *Phys Med*
700 *Biol* **54**, 891-905 (2009).
- 701 30. Matinfar, M. et al. Small animal radiation research platform: imaging, mechanics, control
702 and calibration. *Med Image Comput Comput Assist Interv* **10**, 926-34 (2007).
- 703 31. Matinfar, M., Iordachita, I., Ford, E., Wong, J. & Kazanzides, P. Precision radiotherapy
704 for small animal research. *Med Image Comput Comput Assist Interv* **11**, 619-26 (2008).
- 705 32. Matinfar, M., Iordachita, I., Wong, J. & Kazanzides, P. Robotic Delivery of Complex
706 Radiation Volumes for Small Animal Research. *IEEE Int Conf Robot Autom* **2010**, 2056-
707 2061 (2010).
- 708 33. Wong, J. et al. High-resolution, small animal radiation research platform with x-ray
709 tomographic guidance capabilities. *Int J Radiat Oncol Biol Phys* **71**, 1591-9 (2008).
- 710 34. Armour, M., Ford, E., Iordachita, I. & Wong, J. CT guidance is needed to achieve
711 reproducible positioning of the mouse head for repeat precision cranial irradiation. *Radiat*
712 *Res* **173**, 119-23 (2010).
- 713 35. Ford, E.C. et al. Localized CT-guided irradiation inhibits neurogenesis in specific regions
714 of the adult mouse brain. *Radiat Res* **175**, 774-83 (2011).
- 715 36. Redmond, K.J. et al. A radiotherapy technique to limit dose to neural progenitor cell
716 niches without compromising tumor coverage. *J Neurooncol* **104**, 579-87 (2011).
- 717 37. Fike, J.R., Rola, R. & Limoli, C.L. Radiation response of neural precursor cells.
718 *Neurosurg Clin N Am* **18**, 115-27, x (2007).
- 719 38. Bauer, S., Hay, M., Amilhon, B., Jean, A. & Moyse, E. In vivo neurogenesis in the dorsal
720 vagal complex of the adult rat brainstem. *Neuroscience* **130**, 75-90 (2005).
- 721 39. Hourai, A. & Miyata, S. Neurogenesis in the circumventricular organs of adult mouse
722 brains. *J Neurosci Res* **91**, 757-70 (2013).
- 723 40. Bennett, L., Yang, M., Enikolopov, G. & Iacovitti, L. Circumventricular organs: a novel
724 site of neural stem cells in the adult brain. *Mol Cell Neurosci* **41**, 337-47 (2009).
- 725 41. Gleiberman, A.S. et al. Genetic approaches identify adult pituitary stem cells. *Proc Natl*
726 *Acad Sci U S A* **105**, 6332-7 (2008).

42. Goldman, S.A. & Nottebohm, F. Neuronal production, migration, and differentiation in a vocal control nucleus of the adult female canary brain. *Proc Natl Acad Sci U S A* **80**, 2390-4 (1983).
43. Chow, J.C., Leung, M.K., Lindsay, P.E. & Jaffray, D.A. Dosimetric variation due to the photon beam energy in the small-animal irradiation: a Monte Carlo study. *Med Phys* **37**, 5322-9 (2010).
44. Maeda, A. et al. In vivo optical imaging of tumor and microvascular response to ionizing radiation. *PLoS One* **7**, e42133 (2012).
45. Vasireddy, R.S. et al. Evaluation of the spatial distribution of gammaH2AX following ionizing radiation. *J Vis Exp* (2010).
46. Short, S.C. et al. DNA repair after irradiation in glioma cells and normal human astrocytes. *Neuro Oncol* **9**, 404-11 (2007).
47. Gavrilov, B. et al. Slow elimination of phosphorylated histone gamma-H2AX from DNA of terminally differentiated mouse heart cells in situ. *Biochem Biophys Res Commun* **347**, 1048-52 (2006).
48. Nowak, E. et al. Radiation-induced H2AX phosphorylation and neural precursor apoptosis in the developing brain of mice. *Radiat Res* **165**, 155-64 (2006).
49. Jacques, R., Taylor, R., Wong, J. & McNutt, T. Towards real-time radiation therapy: GPU accelerated superposition/convolution. *Comput Methods Programs Biomed* **98**, 285-92 (2010).
50. Chaichana, K.L., Levy, A.P., Miller-Lotan, R., Shakur, S. & Tamargo, R.J. Haptoglobin 2-2 genotype determines chronic vasospasm after experimental subarachnoid hemorrhage. *Stroke* **38**, 3266-71 (2007).
51. Mah, L.J. et al. Quantification of gammaH2AX foci in response to ionising radiation. *J Vis Exp* (2010).
52. Gage, G.J., Kipke, D.R. & Shain, W. Whole animal perfusion fixation for rodents. *J Vis Exp* (2012).
53. Banath, J.P., Macphail, S.H. & Olive, P.L. Radiation sensitivity, H2AX phosphorylation, and kinetics of repair of DNA strand breaks in irradiated cervical cancer cell lines. *Cancer Res* **64**, 7144-9 (2004).
54. Tryggestad, E., Armour, M., Iordachita, I., Verhaegen, F. & Wong, J.W. A comprehensive system for dosimetric commissioning and Monte Carlo validation for the small animal radiation research platform. *Phys Med Biol* **54**, 5341-57 (2009).
55. Lein, E.S. et al. Genome-wide atlas of gene expression in the adult mouse brain. *Nature* **445**, 168-76 (2007).
56. Tuli, R. et al. Development of a novel preclinical pancreatic cancer research model: bioluminescence image-guided focal irradiation and tumor monitoring of orthotopic xenografts. *Transl Oncol* **5**, 77-84 (2012).

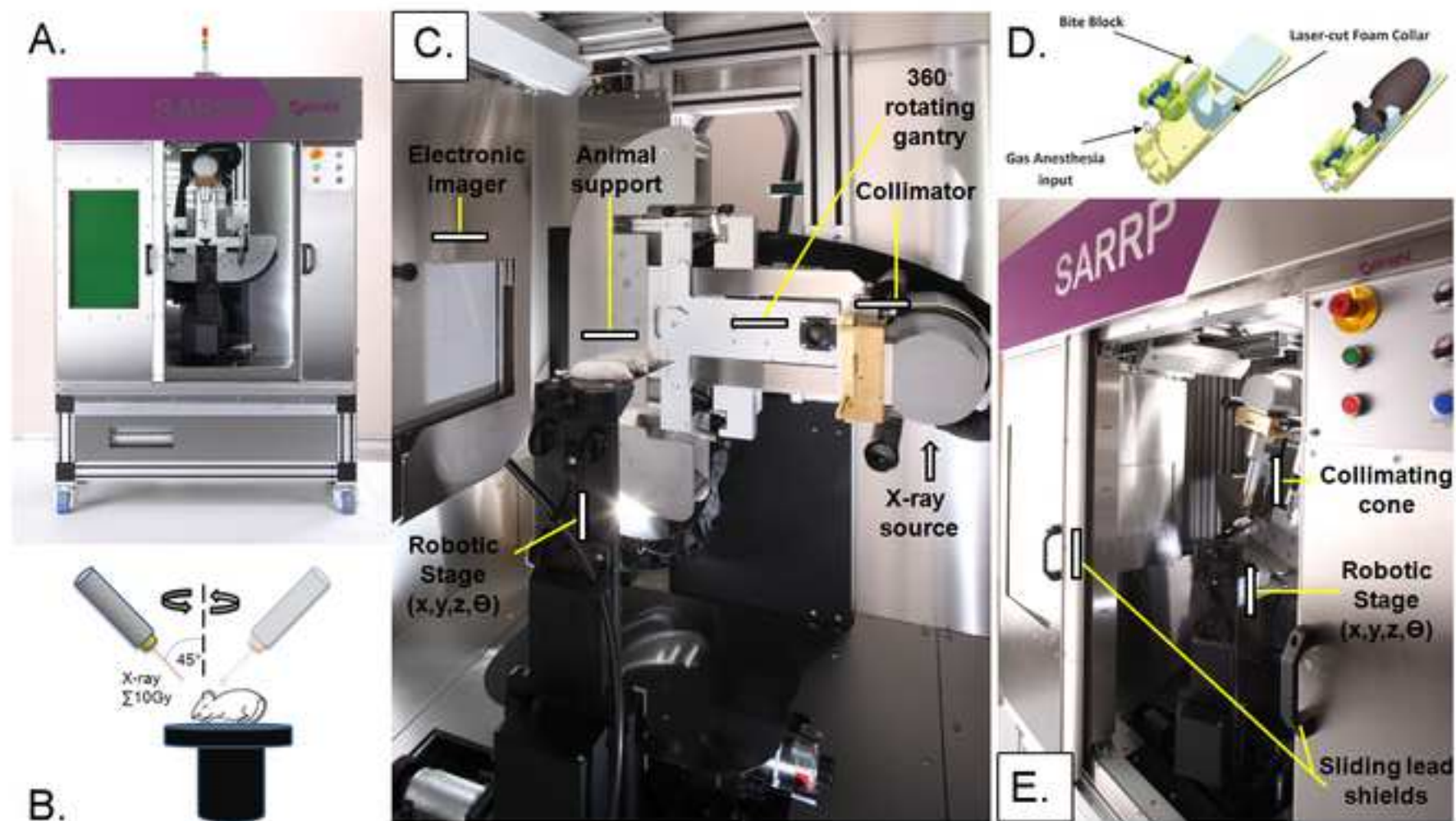
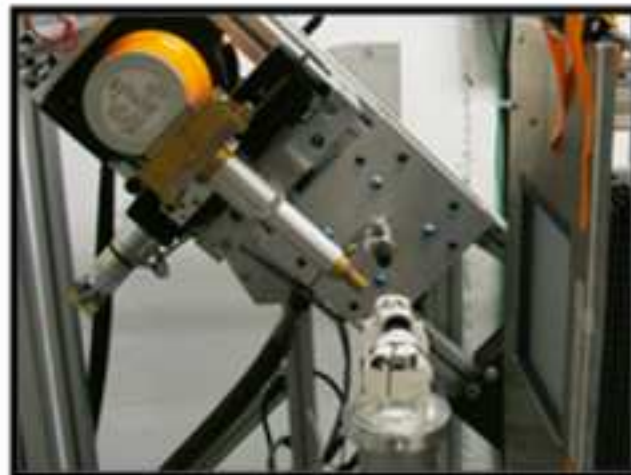


Figure 1.

Figure 2.



**Mice
acclimate**

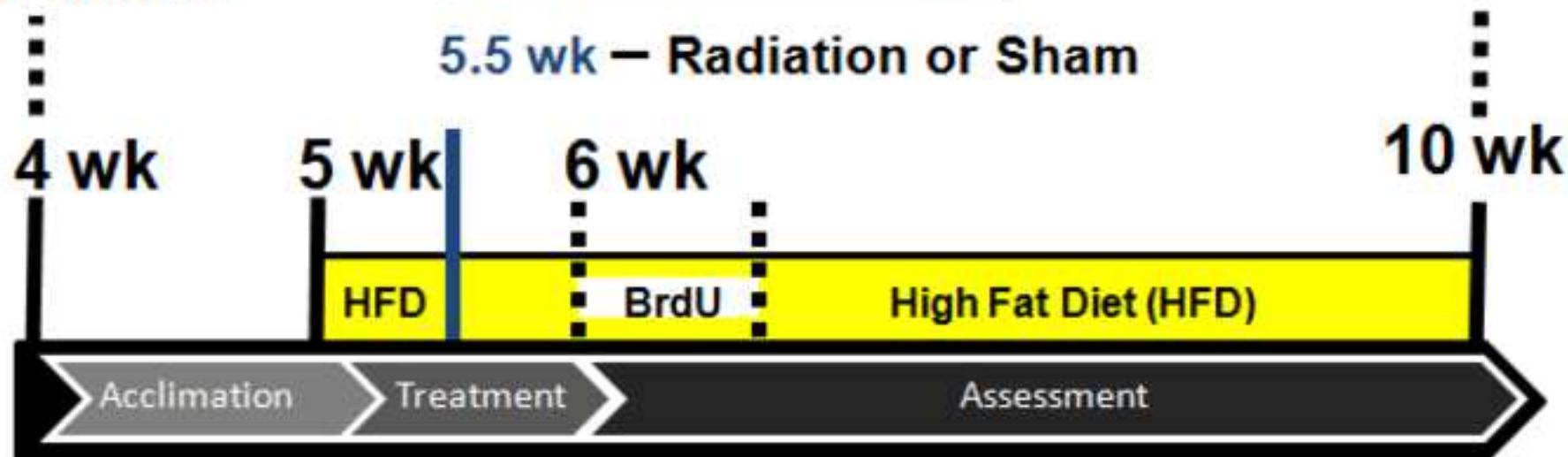


Timepoint analysis:

Neurogenesis

Weight

Metabolism



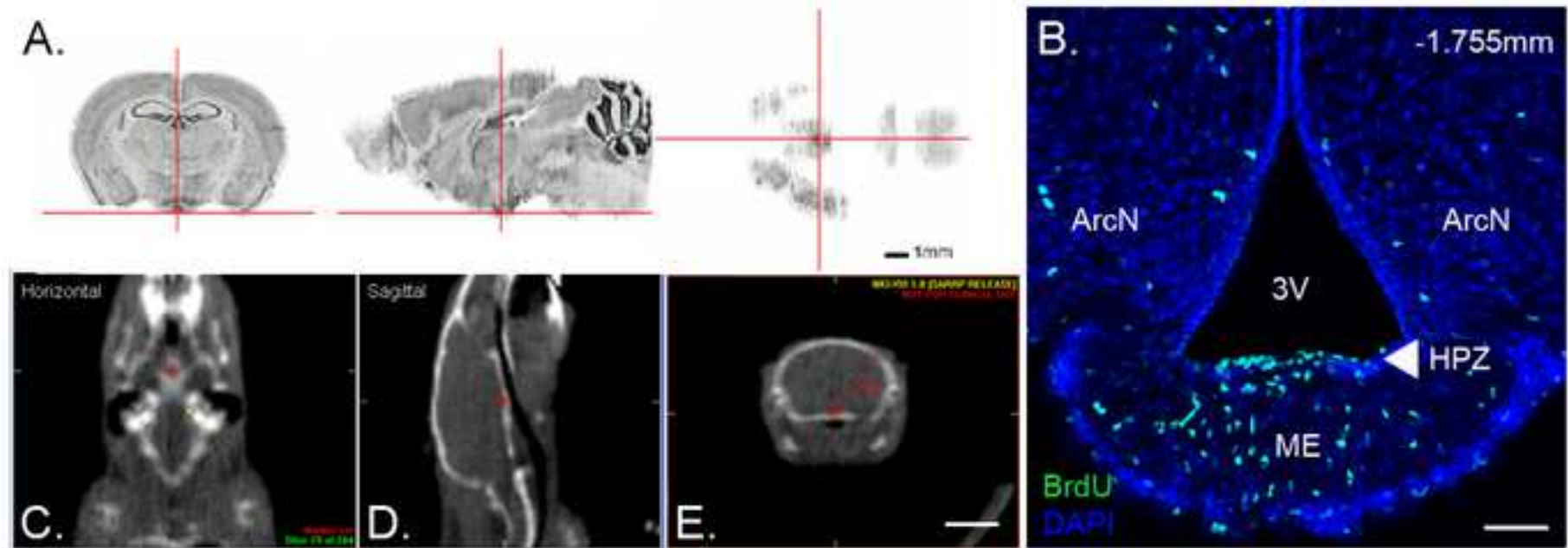


Figure 3.

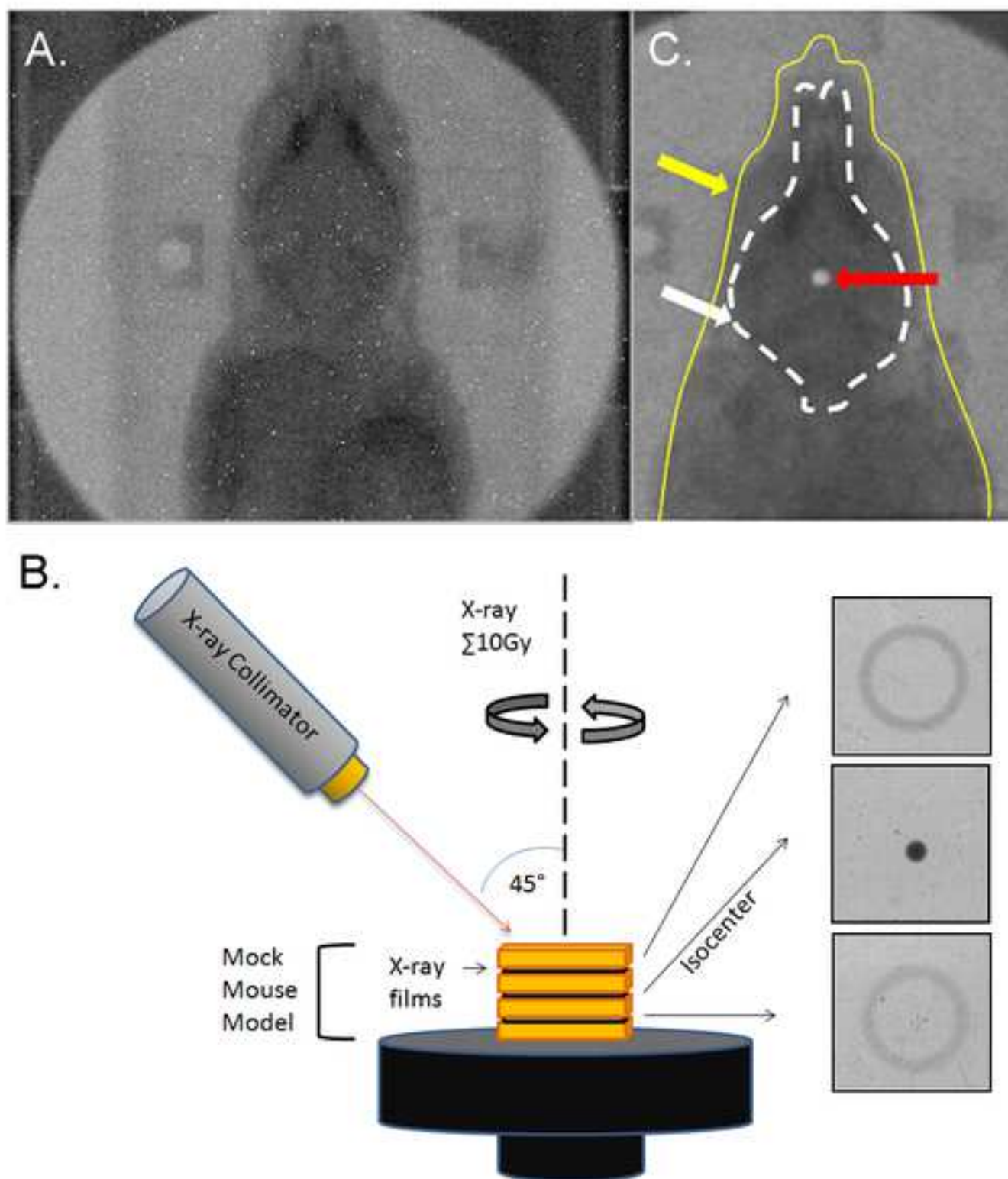


Figure 4.

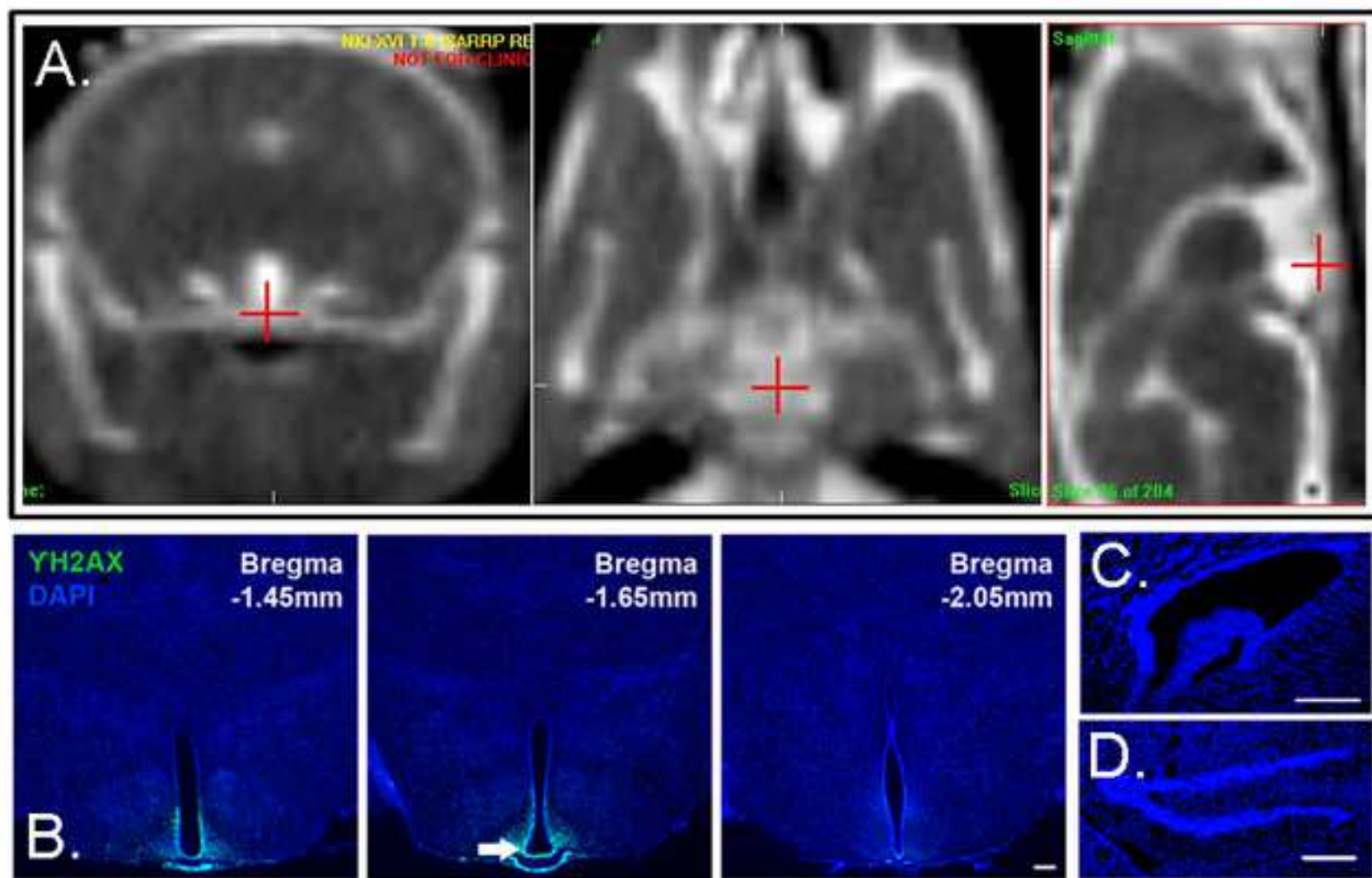
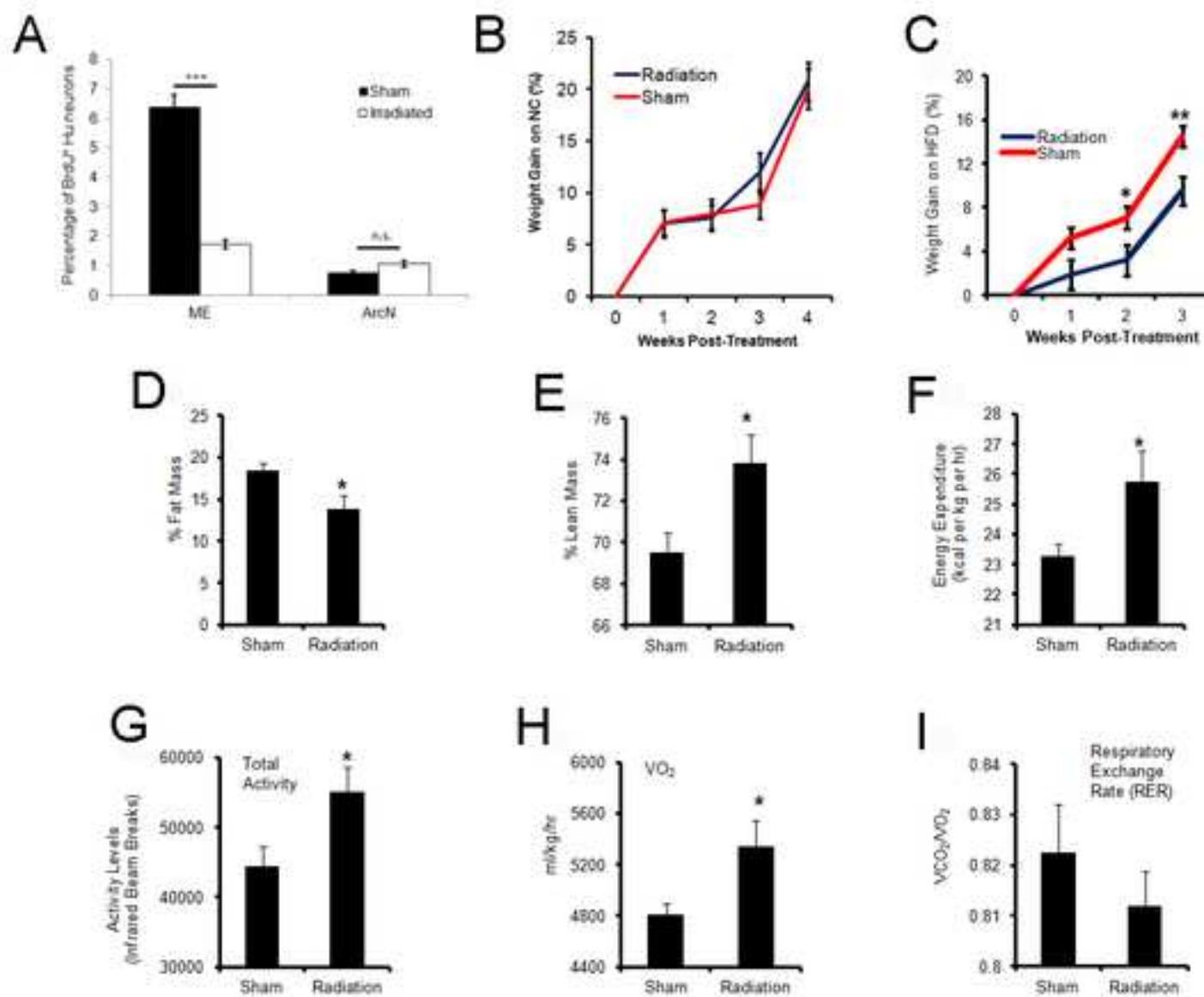


Figure 5.

*Figure 6
[Click here to download high resolution image](#)



I. Troubleshooting Table

Step	Problem	Possible Reason	Solution
1.3	CT image is tilted.	Mouse head is tilted while CT image is being taken.	Align mouse patient’s head so that ears are horizontally level with robotic stage. Tape head down to immobilization bed.
1.3	CT image is fuzzy.	Mouse may have moved while CT image is being taken.	Increase isoflurane gas anesthesia while mouse is on the immobilization bed.
1.4	Difficulty in identifying ROI.	Anatomical region may be difficult to target using cranial landmarks alone (i.e. skull bone).	Use intrathecal iodine contrast (described in Ford <i>et al.</i> , 2011) to enhance visualization of brain ventricles. Identify ROI in relation to brain ventricle position.
1.5	Mouse patient does not awaken following irradiation.	Overdose on anesthesia.	Titrate anesthesia. Lower amount of anesthesia, but enough to keep patient still during irradiation treatment.
1.8	Irradiated region is much larger than ROI.	Radiation beam diameter. may be too big.	Reduce collimator size.
1.8	Irradiated region on GAFchromic film is irregular (not spherical).	Robotic stage may not be rotating smoothly.	Calibrate robotic stage rotation.
2.18	YH2Ax immunostaining does not match desired ROI.	Focal irradiation was not targeted correctly, or is not consistent.	Use additional anatomical landmarks (bone, brain ventricle, etc.) to align radiation beam.

Table of Reagents and Equipment:

Name of the reagent	Company	Catalogue number
SARRP Research Platform	Xstrahl	RS225A
SARRP Irradiation Bunker	Xstrahl	
GAFchromic film	IPS	GAFchromic ETB2
Mouse phantom	Gammex	457
Mouse anti- phospho-histone H2AX Ser139 antibody	Millipore, Inc.	05-636
High-fat rodent diet	Research Diets, New Brunswick, NJ	D12492i
Isoflurane	Baxter Healthcare Corporation	10019-360-40
0.01 M Sodium Citrate	Fisher Scientific	
Superfrost Plus slides	Fisher Scientific	12-550-15
DAPI	Fisher Scientific	
Mounting medium	Fisher Scientific	

Comments
http://www.xstrahl.com/xstrahrs225.htm
Optional, but radiation exposure should be contained with alternative lead shielding
Purchase 0.5x30x30cm solid water slabs from Gammex and cut to desired size.
clone JBW301
60% of the calories as fat, food should be irradiated
1.471g of sodium citrate dissolved in 500ml deionized water

nuclear counterstain

Vectashield or Gelvatol is preferred

ARTICLE AND VIDEO LICENSE AGREEMENT

Title of Article: Probing the functional role of adult hypothalamic neurogenesis by computer tomography image guided focal irradiation

Author(s): Daniel A. Lee, Juan Salvatierra, Esteban Velarde, John Wong, Eric Ford, Seth Blackshaw

Item 1 (check one box): The Author elects to have the Materials be made available (as described at <http://www.jove.com/publish>) via: ☒ Standard Access ☐ Open Access

Item 2 (check one box):

- ☒ The Author is NOT a United States government employee.
- ☐ The Author is a United States government employee and the Materials were prepared in the course of his or her duties as a United States government employee.
- ☐ The Author is a United States government employee but the Materials were NOT prepared in the course of his or her duties as a United States government employee.

ARTICLE AND VIDEO LICENSE AGREEMENT

1. **Defined Terms.** As used in this Article and Video License Agreement, the following terms shall have the following meanings: “**Agreement**” means this Article and Video License Agreement; “**Article**” means the article specified on the last page of this Agreement, including any associated materials such as texts, figures, tables, artwork, abstracts, or summaries contained therein; “**Author**” means the author who is a signatory to this Agreement; “**Collective Work**” means a work, such as a periodical issue, anthology or encyclopedia, in which the Materials in their entirety in unmodified form, along with a number of other contributions, constituting separate and independent works in themselves, are assembled into a collective whole; “**CRC License**” means the Creative Commons Attribution-Non Commercial-No Derivs 3.0 Unported Agreement, the terms and conditions of which can be found at: <http://creativecommons.org/licenses/by-nc-nd/3.0/legalcode>; “**Derivative Work**” means a work based upon the Materials or upon the Materials and other pre-existing works, such as a translation, musical arrangement, dramatization, fictionalization, motion picture version, sound recording, art reproduction, abridgment, condensation, or any other form in which the Materials may be recast, transformed, or adapted; “**Institution**” means the institution, listed on the last page of this Agreement, by which the Author was employed at the time of the creation of the Materials; “**JoVE**” means MyJoVE Corporation, a Massachusetts corporation and the publisher of *The Journal of Visualized Experiments*; “**Materials**” means the Article and / or the Video; “**Parties**” means the Author and JoVE; “**Video**” means any video(s) made by the Author, alone or in conjunction with any other parties, or by JoVE or its affiliates or agents, individually or in collaboration with the Author or any other parties, incorporating all or any portion of the Article, and in which the Author may or may not appear.

2. **Background.** The Author, who is the author of the Article, in order to ensure the dissemination and protection of the Article, desires to have the JoVE publish the Article and create and transmit videos based on the Article. In furtherance of such goals, the Parties desire to memorialize in this Agreement the respective rights of each Party in and to the Article and the Video.

3. **Grant of Rights in Article.** In consideration of JoVE agreeing to publish the Article, the Author hereby grants to JoVE, subject to **Sections 4 and 7** below, the exclusive, royalty-free, perpetual (for the full term of copyright in the Article, including any extensions thereto) license (a) to publish, reproduce, distribute, display and store the Article in all forms, formats and media whether now known or hereafter developed (including without limitation in print, digital and electronic form) throughout the world, (b) to translate the Article into other languages, create adaptations, summaries or extracts of the Article or other Derivative Works (including, without limitation, the Video) or Collective Works based on all or any portion of the Article and exercise all of the rights set forth in (a) above in such translations, adaptations, summaries, extracts, Derivative Works or Collective Works and (c) to license others to do any or all of the above. The foregoing rights may be exercised in all media and formats, whether now known or hereafter devised, and include the right to make such modifications as are technically necessary to exercise the rights in other media and formats. If the “Open Access” box has been checked in **Item 1** above, JoVE and the Author hereby grant to the public all such rights in the Article as provided in, but subject to all limitations and requirements set forth in, the CRC License.

4. **Retention of Rights in Article.** Notwithstanding the exclusive license granted to JoVE in **Section 3** above, the

Author shall, with respect to the Article, retain the non-exclusive right to use all or part of the Article for the non-commercial purpose of giving lectures, presentations or teaching classes, and to post a copy of the Article on the Institution's website or the Author's personal website, in each case provided that a link to the Article on the JoVE website is provided and notice of JoVE's copyright in the Article is included. All non-copyright intellectual property rights in and to the Article, such as patent rights, shall remain with the Author.

5. Grant of Rights in Video – Standard Access. This **Section 5** applies if the "Standard Access" box has been checked in **Item 1** above or if no box has been checked in **Item 1** above. In consideration of JoVE agreeing to produce, display or otherwise assist with the Video, the Author hereby acknowledges and agrees that, Subject to **Section 7** below, JoVE is and shall be the sole and exclusive owner of all rights of any nature, including, without limitation, all copyrights, in and to the Video. To the extent that, by law, the Author is deemed, now or at any time in the future, to have any rights of any nature in or to the Video, the Author hereby disclaims all such rights and transfers all such rights to JoVE.

6. Grant of Rights in Video – Open Access. This **Section 6** applies only if the "Open Access" box has been checked in **Item 1** above. In consideration of JoVE agreeing to produce, display or otherwise assist with the Video, the Author hereby grants to JoVE, subject to **Section 7** below, the exclusive, royalty-free, perpetual (for the full term of copyright in the Article, including any extensions thereto) license (a) to publish, reproduce, distribute, display and store the Video in all forms, formats and media whether now known or hereafter developed (including without limitation in print, digital and electronic form) throughout the world, (b) to translate the Video into other languages, create adaptations, summaries or extracts of the Video or other Derivative Works or Collective Works based on all or any portion of the Video and exercise all of the rights set forth in (a) above in such translations, adaptations, summaries, extracts, Derivative Works or Collective Works and (c) to license others to do any or all of the above. The foregoing rights may be exercised in all media and formats, whether now known or hereafter devised, and include the right to make such modifications as are technically necessary to exercise the rights in other media and formats. For any Video to which this Section 6 is applicable, JoVE and the Author hereby grant to the public all such rights in the Video as provided in, but subject to all limitations and requirements set forth in, the CRC License.

7. Government Employees. If the Author is a United States government employee and the Article was prepared in the course of his or her duties as a United States government employee, as indicated in **Item 2** above, and any of the licenses or grants granted by the Author hereunder exceed the scope of the 17 U.S.C. 403, then the rights granted hereunder shall be limited to the maximum rights permitted under such statute. In such case, all provisions contained herein that are not in conflict with such statute shall remain in full force and effect, and all provisions contained herein that do so conflict

shall be deemed to be amended so as to provide to JoVE the maximum rights permissible within such statute.

8. Likeness, Privacy, Personality. The Author hereby grants JoVE the right to use the Author's name, voice, likeness, picture, photograph, image, biography and performance in any way, commercial or otherwise, in connection with the Materials and the sale, promotion and distribution thereof. The Author hereby waives any and all rights he or she may have, relating to his or her appearance in the Video or otherwise relating to the Materials, under all applicable privacy, likeness, personality or similar laws.

9. Author Warranties. The Author represents and warrants that the Article is original, that it has not been published, that the copyright interest is owned by the Author (or, if more than one author is listed at the beginning of this Agreement, by such authors collectively) and has not been assigned, licensed, or otherwise transferred to any other party. The Author represents and warrants that the author(s) listed at the top of this Agreement are the only authors of the Materials. If more than one author is listed at the top of this Agreement and if any such author has not entered into a separate Article and Video License Agreement with JoVE relating to the Materials, the Author represents and warrants that the Author has been authorized by each of the other such authors to execute this Agreement on his or her behalf and to bind him or her with respect to the terms of this Agreement as if each of them had been a party hereto as an Author. The Author warrants that the use, reproduction, distribution, public or private performance or display, and/or modification of all or any portion of the Materials does not and will not violate, infringe and/or misappropriate the patent, trademark, intellectual property or other rights of any third party. The Author represents and warrants that it has and will continue to comply with all government, institutional and other regulations, including, without limitation all institutional, laboratory, hospital, ethical, human and animal treatment, privacy, and all other rules, regulations, laws, procedures or guidelines, applicable to the Materials, and that all research involving human and animal subjects has been approved by the Author's relevant institutional review board.

10. JoVE Discretion. If the Author requests the assistance of JoVE in producing the Video in the Author's facility, the Author shall ensure that the presence of JoVE employees, agents or independent contractors is in accordance with the relevant regulations of the Author's institution. If more than one author is listed at the beginning of this Agreement, JoVE may, in its sole discretion, elect not take any action with respect to the Article until such time as it has received complete, executed Article and Video License Agreements from each such author. JoVE reserves the right, in its absolute and sole discretion and without giving any reason therefore, to accept or decline any work submitted to JoVE. JoVE and its employees, agents and independent contractors shall have full, unfettered access to the facilities of the Author or of the Author's institution as necessary to make the Video, whether actually published or not. JoVE has sole discretion as to the method of making and publishing the Materials, including,

ARTICLE AND VIDEO LICENSE AGREEMENT

without limitation, to all decisions regarding editing, lighting, filming, timing of publication, if any, length, quality, content and the like.

11. Indemnification. The Author agrees to indemnify JoVE and/or its successors and assigns from and against any and all claims, costs, and expenses, including attorney's fees, arising out of any breach of any warranty or other representations contained herein. The Author further agrees to indemnify and hold harmless JoVE from and against any and all claims, costs, and expenses, including attorney's fees, resulting from the breach by the Author of any representation or warranty contained herein or from allegations or instances of violation of intellectual property rights, damage to the Author's or the Author's institution's facilities, fraud, libel, defamation, research, equipment, experiments, property damage, personal injury, violations of institutional, laboratory, hospital, ethical, human and animal treatment, privacy or other rules, regulations, laws, procedures or guidelines, liabilities and other losses or damages related in any way to the submission of work to JoVE, making of videos by JoVE, or publication in JoVE or elsewhere by JoVE. The Author shall be responsible for, and shall hold JoVE harmless from, damages caused by lack of sterilization, lack of cleanliness or by contamination due to the making of a video by JoVE its employees, agents or independent contractors. All sterilization, cleanliness or decontamination procedures shall be solely the responsibility of the Author and shall be undertaken at the Author's expense. All indemnifications provided herein shall include JoVE's attorney's fees and costs related to said losses or

damages. Such indemnification and holding harmless shall include such losses or damages incurred by, or in connection with, acts or omissions of JoVE, its employees, agents or independent contractors.

12. Fees. To cover the cost incurred for publication, JoVE must receive payment before production and publication the Materials. Payment is due in 21 days of invoice. Should the Materials not be published due to an editorial or production decision, these funds will be returned to the Author. Withdrawal by the Author of any submitted Materials after final peer review approval will result in a US\$1,200 fee to cover pre-production expenses incurred by JoVE. If payment is not received by the completion of filming, production and publication of the Materials will be suspended until payment is received.

13. Transfer, Governing Law. This Agreement may be assigned by JoVE and shall inure to the benefits of any of JoVE's successors and assignees. This Agreement shall be governed and construed by the internal laws of the Commonwealth of Massachusetts without giving effect to any conflict of law provision thereunder. This Agreement may be executed in counterparts, each of which shall be deemed an original, but all of which together shall be deemed to be one and the same agreement. A signed copy of this Agreement delivered by facsimile, e-mail or other means of electronic transmission shall be deemed to have the same legal effect as delivery of an original signed copy of this Agreement.

A signed copy of this document must be sent with all new submissions. Only one Agreement required per submission.

AUTHOR:

Name:

Department:

Institution:

Article Title:

Signature:

Date:

Please submit a signed and dated copy of this license by one of the following three methods:

- 1) Upload a scanned copy as a PDF to the JoVE submission site upon manuscript submission (preferred);
- 2) Fax the document to +1.866.381.2236; or
- 3) Mail the document to JoVE / Attn: JoVE Editorial / 17 Sellers St / Cambridge, MA 02139

For questions, please email editorial@jove.com or call +1.617.945.9051.

MS # (internal use):

April 30, 2013

Dr. Michelle Kinahan, Ph.D.
Science Editor
Journal of Visualized Experiments

Dear Dr. Kinahan,

Thank you very much for your recent letter regarding our manuscript JoVE50716R1 'Functional interrogation of adult hypothalamic neurogenesis with focal radiological inhibition'. We have re-arranged the figures as requested by the reviewers, and addressed all comments below, with our responses in bold font.

Sincerely,

Daniel Lee, Ph.D.

Seth Blackshaw, Ph.D.

Editorial comments:

* All of your previous revisions have been incorporated in to the most recent version of the manuscript. Please download this version of the Microsoft word document from the "file inventory" to use for any subsequent changes.

This has been done.

* Please keep the editorial comments from your previous revisions in mind as you revise your manuscript to address peer review comments. For instance, if formatting or other changes were made, commercial language was removed, etc., please maintain these overall manuscript changes.

This has been done.

* You vary between using OCT and O.C.T. Please make this consistent throughout the manuscript.

This has been corrected. Both OCT and O.C.T. have been replaced with the non-commercial nomenclature of “freezing medium”.

* Please remove commercial language from step 2.17. (Superfrost Plus slides)

This has been removed, and replaced with electrostatically charged microscope slides.

Reviewers' comments:

Reviewer #1:

Manuscript Summary:

This (apparently revised) manuscript is a useful description of Computer tomography-guided focal irradiation (CFIR) of defined regions in the mouse brain. Specifically, the authors focus on the hypothalamic median eminence, for which they have recently demonstrated increased production of new neurons in response to a high-fat diet. Such and related experiments often require local suppression of neurogenesis and irradiation is often a method of choice. Problem is that in most cases large areas of the brain become exposed to radiation, thus bringing into question the relevance of the response. This problem becomes particularly acute for the studies of hypothalamic neurogenesis, where neighboring pituitary may become exposed to radiation and change the hormonal status of the entire organism. The authors present a detailed description of a small animal radiation research platform that they have developed (there are similar devices available commercially and their use may also benefit from the detailed description of the procedure in the current manuscript). The procedure is described clearly and fully, starting with preparing mice for the experiments and ending with the tests for the radiation effects, such as gamma-H2AX histone immunocytochemistry. The importance of the manuscript is in clear description of a method that has value beyond the studies of the hypothalamic neurogenesis per se and may be adjusted for irradiating other subregions of the rodent brain. The manuscript is written clearly (line 152 - should "control" be "controlled"?) and the illustrations are relevant to the material. **(line 152 has now been corrected)**. Overall, this is a useful methods paper which should help researchers in the field. My only request would be to provide a better discussion of how this protocol can be adjusted for other models of CT-guided irradiation setups, because that will increase the range of researchers interested in the protocol; at this point the use of this technique is essentially limited to the authors' research groups with an access to a unique device.

We thank the Reviewer for his/her positive evaluation. To address the Reviewer's request, we have now discussed more extensively how this CFIR protocol can be used to provide conceptual advances in other research areas. Specifically, we discuss how CFIR could be used to evaluate the function of progenitor populations that have been suggested in other circumventricular organs such as the area postrema (Bauer et al., 2005; Hourai and Miyata, 2013), subfornical organ (Bennett et al., 2009; Hourai and Miyata, 2013), and the pituitary (Gleiberman et al., 2008). We also discuss how using this technique could address longstanding questions of the role of neurogenesis in maintaining birdsong, which have been hampered by the ability to specifically inhibit neurogenesis in specific brain regions relevant to birdsong. It is our hope that publicizing this methodology that will allow researchers outside of our immediate research focus to extend this technique to provide conceptual advances in their own field.

Reviewer #2:

Major Concerns:

This is an innovative well-written manuscript.

We thank the Reviewer for his/her positive evaluation.

The following issues should be addressed.

1. It is unclear why female mice and relatively young mice are being used. Does this not work with older and male mice?

This CFIR protocol works with older mice, as well as male mice. In our previous work using this technique, we performed this protocol in 8 week old male mice. In Ford *et al.*, 2011, we highlight using arc targeting to focally irradiate the hippocampal subgranular zone in that publication. This manuscript goes into greater description on how to irradiate a limited focal region, and works on all ages in principle. Furthermore, as we have shown from our previous work, CFIR works on both sexes (Lee *et al.*, 2012; Ford *et al.*, 2011).

2. The anesthesia might modulate the effects of irradiation. That should be discussed.

This problem is not well studied. The radiation response of tissues probably does change in response to anesthesia due to temperature and oxygenation effects. An over-response has been shown in animal tumor models. For clinical purposes where patients are treated under anesthesia the response is assumed to be minimal. The key here, though, is that we are using large localized doses for ablative purposes. If there is an over response due to anesthesia it would not impact the experiment.

3. Recent evidence suggests that DNA double strand breaks occur even if mice explore a novel environment. Therefore, using this method to determine the selectivity of radiation might often not be possible.

There are other methods such as immunohistochemistry against 53BP1, but similar issues exist there. The number of breaks after irradiation is much higher than the background level referred to here. The purpose of the present experiment is to visualize the location of the irradiated area which is readily accomplished.

4. It seems important to include the regular diet in the context of irradiation as well to determine if the effects seen are only seen when mice are on a HFD.

This is now included alongside the HFD data (see revised Figure 6B). Indeed, we have only seen these effects on weight and metabolism with HFD-fed mice or with mouse models of metabolic disorders.

Reviewer #3:

This is a nice study demonstrating the focal irradiation of hypothalamus neurogenic zones under CT guidance. This approach has important implications on investigations of other neurogenic regions as well.

We thank the Reviewer for his/her interest and positive evaluation.

Major Concerns:

1. For the protocol, draw it out with squares representing each steps in sequence. This is better than text.

In keeping with the suggested guidelines of the JOVE instructions to authors, this has been kept as text. Similarly, all figures have been kept as layered psd file format so that the JOVE editorial staff can re-arrange the subfigures into square panels during the video editing process. If the editor would like us to change the protocol into squares, please do let us know. We thank the reviewer for this constructive suggestion.

2. Make a "TROUBLE shooting" PANEL for all potential problems during this experiment. Check Nature protocol papers.

This has now been included. We list the most common problems that we encountered initially, or that we envision others would encounter while performing this protocol. There are, of course, a number of issues that may arise related to hardware and software issues that are specific to whatever radiological research platform the end-user selects. In those cases, we would suggest they refer to the technical manuals provided at the installation of those devices.

3. Figure 1,2 can be put together. Figure 6 is important, but it is too few data to stand alone as one figure. The author may integrate this into other figures, or include example pictures at the 3rd Ventricular zone with BrdU labeling.

Figure 6 has now been integrated with Figure 7. This has been updated in the text as well. However, in keeping with editorial suggestions on the JOVE website, Figure 1 and 2 has been kept separate.

4. Please discuss the previous failures or mistargeting effects. As shown in Figure 5B, the bottom region of the brain (optic tract??) also demonstrated irradiation effects. Will this harm the vision of the animal, for example?

At the doses used here, no frank radiation injury is expected to well-differentiated normal tissue. The dose to the optic nerve for example would not visually impair the mouse. Furthermore, the irradiated zone includes very little of the optic nerve, and ongoing rates of cell proliferation in adult optic nerve are very small in any case.

In addition, it is the region at the very apex of these radiological beams that demonstrate substantial inhibition of cell proliferation. In our previous study (Lee *et al.*, Int J Dev Neuro, 2012), where we target the median eminence (apex), we find no defect in neurogenesis in the adjacent arcuate nucleus, even though lower levels of gamma H2AX immunostaining are also detected there immediately following irradiation.

Minor Concerns:

Spelling errors.

line 186: 5.5-10 week should be "weeks" ? (see line 203, 205) – **this has been changed.**

line 196: the, ventrobasal should be "the ventrobasal" - **this has been changed.**